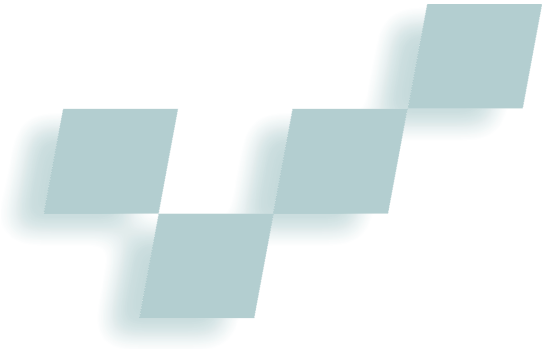

# Surface Acoustic Wave Tactile Display

**Takaaki Nara, Masaya Takasaki, Taro Maeda, Toshiro Higuchi, Shigeru Ando, and Susumu Tachi**
*University of Tokyo, Japan*

**We propose a tactile display using surface acoustic waves. We can continuously change the fineness of the surface's grain by controlling the SAWs' burst frequency.**

Developing realistic tactile displays for virtual reality has been challenging. Tangible displays are increasingly important interfaces not only for augmenting the reality of computer graphics but also for conveying graphical information to persons with visual impairments. Researchers have used various actuators for displays such as miniature loud speakers,[1] a pin array,[2] pneumatic actuators,[3] and ultrasonic vibrators.[4] Researchers have also proposed methods based on the processing properties of human tactile information. Humans feel tactile sensations via mechanoreceptive units that are classified into four categories—rapidly adapting I and II (RAI and RAII) and slowly adapting I and II (SAI and SAII), whose end organs are Meissner corpuscles, Pacinian corpuscles, Merkel cell-neurite complexes, and Ruffini endings, respectively.[5] Shinoda developed a tactile display that stimulates each mechanoreceptor selectively, using the human skin's elastic transfer property.[6]

However, because the researchers didn't clarify the parameters that characterize roughness, rigidity, and material quality, they weren't able to show a principle for systematic control of tactile sensations by the previously mentioned devices. This resulted in using ad-hoc stimulation in the displays for creating particular sensations. Furthermore, the researchers didn't consider the mechanisms for the mechanoreceptors' motion.

Clarifying the receptors' mechanical properties lets us obtain a more effective method for stimulating the processing system of human tactile sensation. Thus, in this article, we first analyze which skin deformations the RA-type mechanoreceptors detect. Based on the result of the analysis, we clarify a flow of tactile information from the objects' parameters to the receptors' deformation, which leads to a proposal for the surface acoustic wave (SAW) tactile display.

## Models of mechanoreceptors and skin

In this section, we analyze the properties of mechanoreceptors and skin from the viewpoint of skin deformation to which the mechanoreceptors are sensitive. This analysis suggests the principle of the SAW tactile display.

### *Meissner and Pacinian corpuscles*

Meissner corpuscles, which have a relatively low characteristic frequency of about 40 Hz, are localized in the papillary dermis with a height of around 150 μm and a diameter of 40 to 70 μm. A structural feature is their coiled axons[7] on which $Ca^{2+}$ ion channels exist.[8] Guharay et al.[9] showed that a probability of general mechanosensitive ion channels being open depends on the energy of deformation expressed as $U = K/2 \cdot (\Delta A/A)^2 \cdot A$, where $K$ is the channel's elastic modulus and $A$ is the channel's size. Thus, we must analyze the axon surface's deformation when stress by skin is applied to the corpuscles.

**Transmission of deformation by a coil.** We first clarify a coiled structure's mechanical properties. As Figure 1 shows, we set an $x$ axis along the wire of the coil and $y$, $z$ axes in a section of the wire. When we apply normal (Figure 1a) and shear (Figure 2a) stresses to the top and bottom of the coil, a torsional moment $M_x$ and bending moments $M_y$, $M_z$ are applied to the section of the wire in Figures 1a and 2a. Note that only the torsional moment is generated when we apply $P$ to the coil. As a result, only shear deformation on a coil surface is generated when we apply normal stress to the coil (Figure 1b), while stretch deformation—in addition to shear deformation—is created on the surface when we apply shear stress to the coil (Figure 2b).

Because activating the axon depends on the ratio of change of the channel size, the shear stress to the coil—which generates stretch deformations on the coil surface—changes the surface's size to increase the probability of the channel being open. Therefore, we hypothesized that the coiled axon of Meissner corpuscles is sensitive to shear stress in the skin. To verify this


0272-1716/01/$10.00 © 2001 IEEE

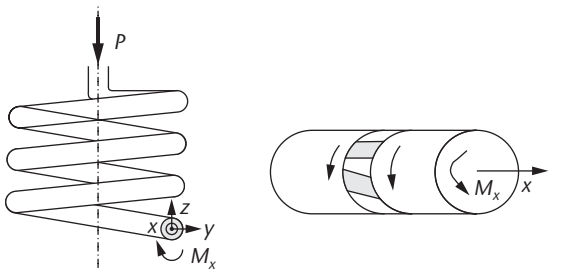


(a) (b)

**1 When we apply vertical stress to the coil, (a) a torsional moment $M_x$ is generated at a cross-section of the wire, (b) which creates a shearing deformation at the wire's surface.**

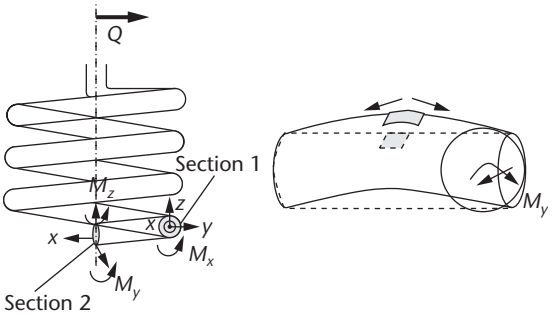


(a) (b)

**2 When we apply shear stress to the coil, (a) in addition to a torsional moment $M_x$, bending moments $M_y$, $M_x$ are generated at cross-sections of the wire, (b) which creates shearing and stretch deformations at the wire's surface.**

statement, we show next that we can derive the corpuscles' tuning curve on the basis of the coiled axon's shearing resonant character.

**Dynamic properties of a coil.** We can express a coil's longitudinal resonant frequency of $\omega_z$ and a shearing resonant frequency of $\omega_z$ as

$$\omega_z = \frac{d}{nD^2}\sqrt{\frac{\mu}{2\rho}}, \quad \frac{\omega_x}{\omega_z} = \sqrt{\frac{2(1+\nu)}{1+12(2+\nu)\left(\frac{H}{D}\right)^2}} \tag{1}$$

where $d$ is the diameter of the coil's wire, $\mu$ is the rigidity of the wire, $\rho$ is the density of the wire, and $\nu$ is the Poisson's ratio of the wire. Assuming that $\nu$ is approximately 0.5 and $H/D = 150\ \mu m/50\ \mu m$ as in the Meissner corpuscles,

$$\frac{\omega_x}{\omega_z} = \frac{1}{10} \tag{2}$$

Thus, we can consider that the corpuscles' characteristic frequency derives from the shearing resonant frequency as the coiled axon's minimum resonant frequency. In fact, with parameters observed in medical experiments,[7] $\omega_x/2\pi = 44$ Hz, which corresponds to the real characteristic frequency. Moreover, we can derive the tuning curve from the energy of the coil's shearing deformation, which depends on the shear stress in the skin, as Figure 3 shows. Although our analysis here is too simplified and we should further investigate the role of the Schwann cells and the collagen fibers of the corpuscles for detecting normal stress of the skin, our discussion suggests that Meissner corpuscles might easily detect shearing, equivoluminal deformation in the skin.

Also, as for Pacinian corpuscles (the other RA-type mechanoreceptors), we've shown that the structure of the layered lamellae of Pacinian corpuscles might easily detect skin's equivoluminal deformation with a coupled pendulum model verified by deriving tuning curves.[11] In this way, we suggest that dynamic, shear, equivoluminal deformation inside skin is an important factor for stimulating the RA-type mechanoreceptors.

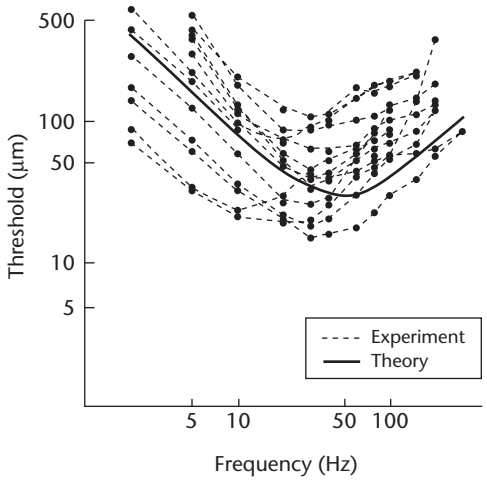


**3 The tuning curve of the Meissner corpuscles.[10] Assuming that the Meissner corpuscles detect shear stress of the skin, we can derive the tuning curve from the shearing resonant characteristic of the coiled axon. We drew the experimental curves according to the Talbot's data.[10]**

### *Equivoluminal deformation as invariant*

In this section, we investigate the equivoluminal deformation's meaning from the viewpoint of an invariant of skin deformation. Although here we consider an idealized skin model of an isotropic, homogeneous, and infinite elastic body, this discussion shows important components of deformation for mechanoreceptors in tactile displays. We can completely express an elastic body's deformation by the stress tensor's six components. However, the tensor's components depend on the coordinates' direction. Thus, unless mechanoreceptors with spherical asymmetric shapes are set in a uniform direction in skin or a central nerve system calibrates the directions of all the mechanoreceptors, the brain can't process tensor components consistently from spatially distributed mechanoreceptors. Actually, the mechanoreceptors aren't always distributed in the uniform direction in skin. Then,

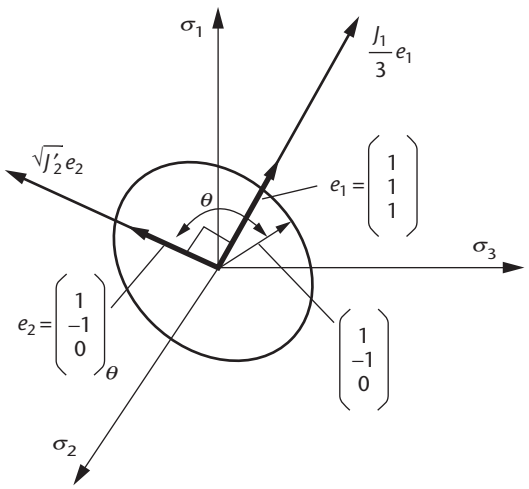


**4 Orthogonal decomposition of a principal stress. Any deformation is decomposed into dilatation and distortion according to the decomposition of a principal stress into a mean stress component and an octahedral shear stress component.**

let's consider a diagonal component of deformation of

$$\begin{bmatrix} \sigma_x & \tau_{xy} & \tau_{xz} \\ \tau_{xy} & \sigma_y & \tau_{yz} \\ \tau_{xz} & \tau_{yz} & \sigma_z \end{bmatrix} = Q^{-1} \begin{bmatrix} \sigma_1 & 0 & 0 \\ 0 & \sigma_2 & 0 \\ 0 & 0 & \sigma_3 \end{bmatrix} Q \tag{3}$$

that the central nerve system can detect in spite of the mechanoreceptors' directions. The eigen values $\sigma_1$, $\sigma_2$, $\sigma_3$—the principal stress—are independent of the coordinates' direction. Here, we can decompose a vector composed of ($\sigma_1$, $\sigma_2$, $\sigma_3$) as

$$\begin{bmatrix} \sigma_1 \\ \sigma_2 \\ \sigma_3 \end{bmatrix} = \frac{J_1}{3} \begin{bmatrix} 1 \\ 1 \\ 1 \end{bmatrix} + \sqrt{J_2'} \begin{bmatrix} 1 \\ -1 \\ 1 \end{bmatrix}_\theta \tag{4}$$

where $J_1$, $J'_2$ are the first-order stress invariant and the second-order stress deviation invariant, respectively. The first term of (1, 1, 1) corresponds to an isotropic deformation with a coefficient

$$\frac{J_1}{3} = \frac{\sigma_1 + \sigma_2 + \sigma_3}{3} \tag{5}$$

which is proportional to dilatation. On the other hand, the second term of $(1, -1, 0)\theta$, which is rotated from (1, −1, 0) with an angle of $\theta$ on a plane perpendicular to (1, 1, 1), corresponds to equivoluminal deformation with a coefficient

$$\sqrt{J_2'} = \sqrt{\frac{3}{2}} \tau_{oct} \tag{6}$$

where $\tau_{oct}$ is an octahedral shear stress. As Figure 4 shows, these two terms are perpendicular in the vector space composed of principal stress. Thus, if the central nerve system can detect invariants ($J_1/3$, $\sqrt{J'_2}$) in the elastic skin, it can realize an effective sensing of principal stress that's independent of the mechanoreceptors' direction because they're the independent components of an orthogonal decomposition. In our analysis in the previous section, we expressed modes that the Meissner and Pacinian corpuscles are sensitive to as

$$\tau \begin{bmatrix} 0 & 1 \\ 1 & 0 \end{bmatrix}, \quad \sigma \begin{bmatrix} 1 & 0 \\ 0 & -1 \end{bmatrix} \tag{7}$$

in 2D problems, where $\tau$ and $\sigma$ are proportional to $\sqrt{J'_2}$ representing equivoluminal deformation. Also, as for the SA-type mechanoreceptors, Srinivasan[12] showed an interesting result that strain energy density,

$$\phi = \frac{1}{4\mu_s} \left( \frac{1-2\nu_s}{3(1+\nu_s)} J_1^2 + 2J_2' \right) \tag{8}$$

where $\nu_s$ is Poisson's ratio and $\mu_s$ is rigidity of skin, is a candidate to be the relevant stimulus for SAI.

The relevant stimulus for the RA-type mechanoreceptors should be investigated by physiological experiments. However, our discussion suggests the importance of equivoluminal deformation, which is easily detected by the RA-type mechanoreceptors, as an independent component of skin deformation. Next, we investigate how equivoluminal deformation inside skin is generated in active touch.

### *Skin distortion in active touch*

We analyzed contact and relative motion between the finger and an object by a spring ($k$)–mass ($m$) model of the finger moving on an object's Gaussian surface with constant velocity ($U$) of exploration.[13] By the Hertz contact theory, we can approximately express the normal stress $p$ and shear stress $q$ to the skin surface generated at the positions of the projections as

$$q = s + \frac{\sigma}{\beta} p, \; p = \frac{E}{\pi} \cdot \frac{\sigma}{\beta} \tag{9}$$

where $E_o$, $E_s$ is Young's ratio of the object and the skin, respectively; $\nu_0$ is Poisson's ratio of the object; $1/E = (1-\nu_s^2)/E_s + (1-\nu_o^2)/E_o$, $s$, and $s'$ are the skin's static and kinetic shear strength; $\sigma$ is the topography's standard deviation; and $\beta$ is the topography's mean radius of projections. Then, during the exploration, we can show that the stress $q$ and $p$ to the skin surface can be temporally vibrated in a stick-slip motion with a stick-slip frequency $f_{ss}$ expressed as

$$f_{ss}^{-1} = \frac{2}{\omega_0} (\pi - \tan^{-1} R + R) \tag{10}$$

$$R = \frac{(\mu_s - \mu_c) P}{m \omega_0 U} \tag{11}$$

$$\mu_s - \mu_c = \frac{\pi (s - s') \beta}{E_\sigma}, \; \omega_0 = \sqrt{\frac{k}{m}} \tag{12}$$

where $P$ is a total normal pressure by the skin. Figure 5 shows the relationship between an object's parameters and the stick-slip frequency, which is a key relationship for displaying material quality in the next section. As an example, we drew Figure 5 with $P = 1$ Newton (N), $m =$ 1 gram, $k = 500$ N/m, and $U = 4$ cm per second.

Under these boundary conditions at the skin surface, let's consider deformation inside the skin. At the moment of the shift from the stick state to the slip state, normal and shear stress begins to move suddenly on the skin surface. As a result, elastic waves are created inside the skin, and these are dominant deformations because amplitudes are much greater than the stationary deformation generated during the stick state or the slip state. Now, consider skin deformation with a 2D elastic skin model when normal and shear stress that vary with time as the Heaviside unit-step function is applied to the skin surface. Remarkably, the polarity of the S-wave's amplitudes, which are much larger than the P-wave's amplitude, turns over along the skin surface by the normal stress in contrast to the constant polarity by the shear stress.[11] As a result, the S-waves by many normal sources distributed over the skin surface are canceled, while the S-waves by the distributed shear sources become large because of a constructive interference. In this way, we can show that primal surface stress, which creates dominant deformation inside the skin, is dispersed shear stress. The following represents our analysis, which we summarized as a flow of tactile information:

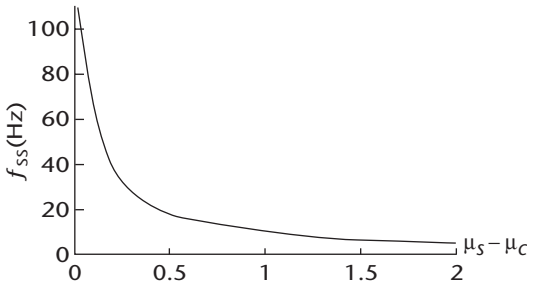


**5 Relationship between a parameter of $\mu_s - \mu_c$ and a stick-slip frequency.**

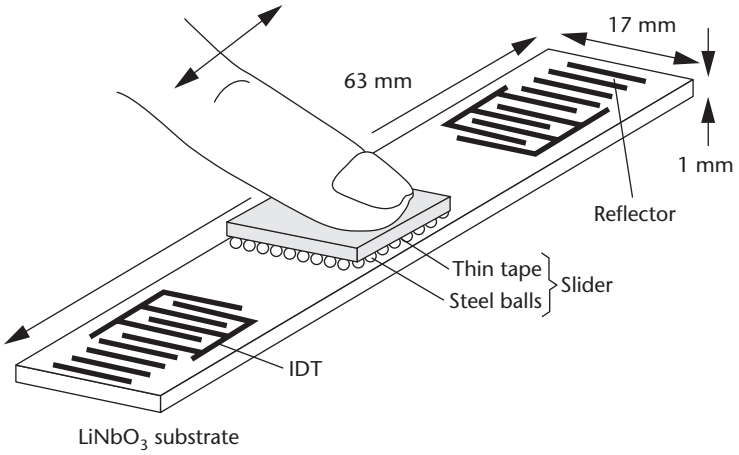


**6 Schematic description of the SAW tactile display.**

1. Parameters of the object to be touched and the motion of an active touch: $(E_0, \nu_o, \sigma, \beta) \times (P, U)$.
2. Stress on the skin surface:
   Dispersed sources of shear stress, $q = s + E/\pi \cdot (\sigma/\beta)^2$, and stick-slip frequency, $f_{ss} = 1/T_{ss}$ in Equations 10 through 12.
3. Equivoluminal deformation inside the skin due to the constructive interference.
4. Meissner and Pacinian corpuscles: Detection of the equivoluminal deformation. The ratio of the contribution of both corpuscles is changed by $f_{ss}$.

## SAW tactile display

In this section, we develop the SAW tactile display, which can effectively stimulate the mechanoreceptors inside skin. We show an experiment of controlling fineness of grain and its several applications.

### *Shear sources method*

Based on our discussion in the previous section, we can derive the prerequisites for tactile control—especially for stimulating the RA mechanoreceptors—as follows:

- Sources of shear stress should be applied to the skin surface to create equivoluminal distortion detected by the mechanoreceptors.
- The sources of shear stress can be spatially dispersed on the finger surface.
- The sources of shear stress can be temporally modulated with a stick-slip frequency $f_{ss}$ determined by the parameters of the object to be displayed.

Although many previous tactile displays have used stimuli perpendicular to the skin surface,[1-3] several displays can control parallel force to the skin surface by using ultrasonic vibration[4] or piezoelectric actuators.[14] As used in S-wave gnerators in geophysical prospecting, a method using phase-inverted perpendicular vibrations[6] is also equal to controlling shear stress to the skin.

However, because relative motion between the skin and real objects hasn't been analyzed until now, it's unclear how to temporally modulate shear stress. It's also impossible to control a sensation of roughness systematically as though diameters of small projections on a rough surface change continuously. We propose to use SAWs to generate sources of shear stress that satisfy the three prerequisites for tactile control.

### *Device*

SAWs have recently attracted attention for sources of driving force for linear motors[15] in addition to their practical application as a filter for telecommunication equipment. We use SAWs for tactile control.

Figure 6 schematically shows the SAW tactile display's structure. On a Lithium Niobate ($LiNbO_3$) 128-degree Y-cut substrate whose size is 17 mm × 63 mm × 1 mm, alternating voltage to an interdigital transducer (IDT) generates a SAW. A SAW's wavelength is about 265 μm with the driving frequency of 15 MHz. One of the prominent advantages of the display is the substrate's thin-

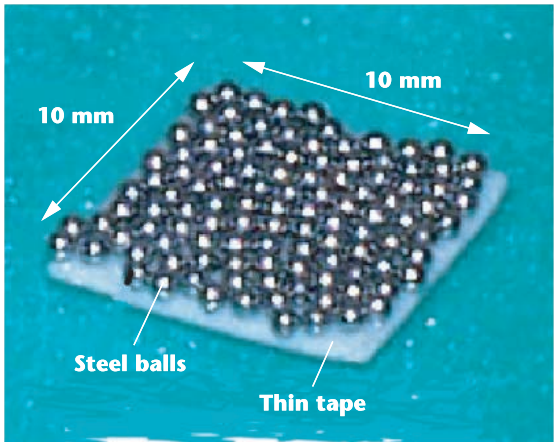


**7** Detail of the slider.

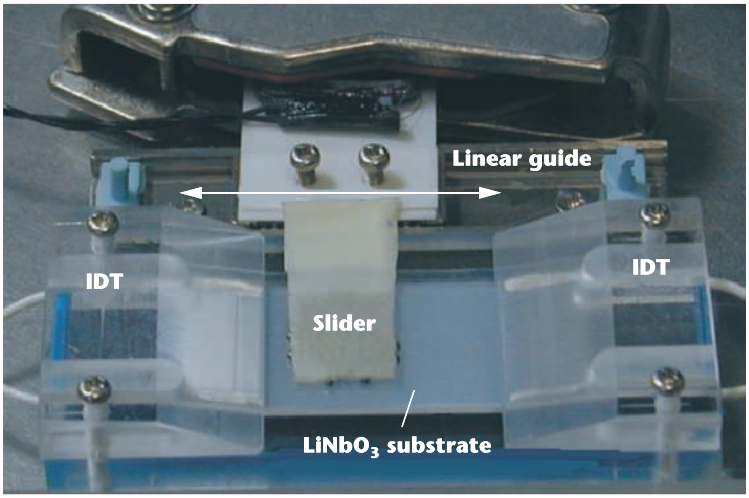


**8** The SAW tactile display.

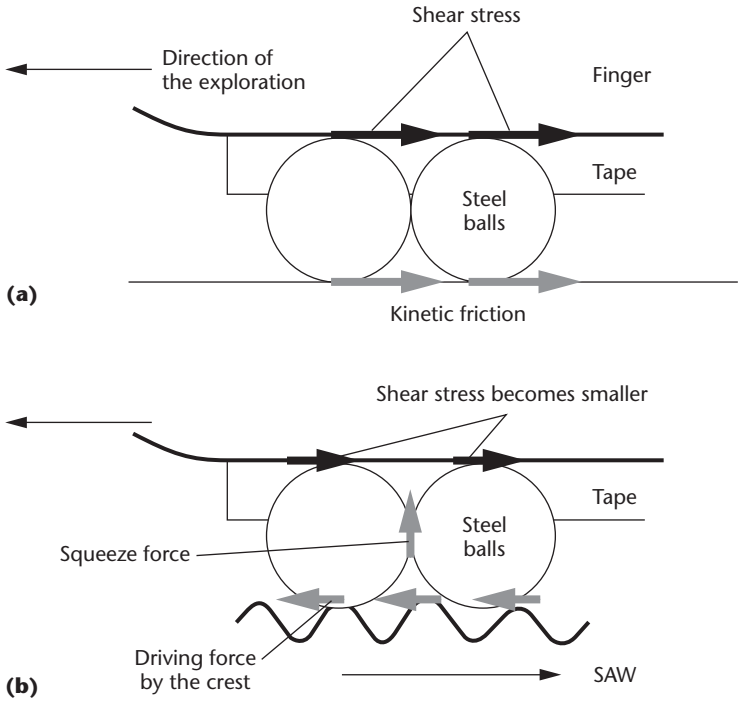


**9** Generation of sources of shear stress that can be modulated temporally by burst waves of SAW.

ness (1 mm) for creating stimuli to the finger.

We placed IDTs at both ends of the substrate. To generate progressive waves, we applied an alternating voltage to one side of the IDTs. To generate standing waves, we applied the voltage to both sides of the IDTs and set open-metal-strip arrays (OMSA) after the IDTs as reflectors.

In our tactile display, users can explore the substrate with a slider shown in Figures 7 and 8. The slider has approximately 100 steel balls with a diameter of 800 µm on a thin tape. We chose to use a slider because of the following:

- By pressing steel balls with the finger, a driving force can be effectively transmitted to the finger.
- Steel balls can provide distributed points to which stress is applied on the finger surface, assuming that the tape is satisfactorily thin and soft.

### *Principle*

Here we describe the principle for generating sources of shear stress that are distributed spatially and modulated temporally.

When users explore the substrate without SAWs with their fingers—via the slider—kinetic friction by the substrate is applied to the steel balls, thus creating sources of shear stress on the fingers' surface at the positions of all the steel balls distributed spatially (Figure 9a).

By generating SAWs, we can descrease the friction between the steel balls and the substrate compared to the substrate without SAWs because there's a

- decrease in contact time between the balls and the substrate,
- squeeze-film effect by the air that exists between the balls and the substrate, and
- parallel movement of the wave crest (only in using progressive waves).

As a result, when we either generate a progressive or standing SAW in the substrate, shear stress to the skin becomes smaller (Figure 9b) than shear stress without a SAW. Thus, by using a burst waves of SAW, we can modulate the sources of shear stress applied to the skin surface with a burst frequency. The moment when the wave suddenly appears corresponds to the moment when the stick state changes into the slip state because the friction suddenly

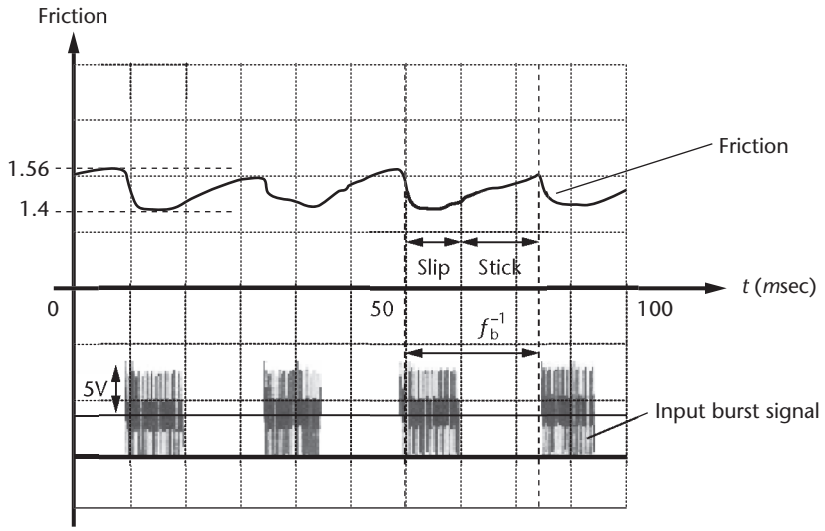


**10** **Experimental data of friction between the substrate and the slider. Generating SAWs reduces friction. Thus, a burst standing SAW can create a virtual stick-slip vibration of friction.**

decreases. Therefore, we can control the stick-slip frequency virtually by changing the burst frequency. In this way, we obtain distributed sources of shear stress that are modulated with a stick-slip frequency determined by the object's solidity and roughness.

## Experiments

We performed experiments to control the roughness of objects by changing the frequency of the modulation of the shear stress' distributed sources.

### *Generation of virtual stick-slip*

Figure 10 shows an input signal of a burst wave to the IDTs and the resulting temporal friction change. The burst wave has a carrier frequency of 15 MHz and a duty ratio of 40 percent. The input power is 2 to 3 watts for standing waves and 100 watts for progressive waves. In this experiment, we used standing waves. We measured normal pressure to the slider and friction between the slider and the substrate by strain gauges force sensors. In the curve of the measured data of friction, we confirmed a 89 percent decrease of friction from 1.56 N to 1.4 N under a normal pressure of 11.7 N during the generation of a SAW. This is a virtual stick-slip vibration of friction. The burst frequency, denoted $f_b$, is a variable for controlling a tactile sensation in the next section.

### *Obtained tactile sensation*

First of all, when the finger stops on the substrate, a user doesn't feel the vibration of the standing SAW perpendicular to the skin surface at all. However, exploring the substrate generates a sensation of roughness that's variable by the burst frequency $f_b$ as follows. When $f_b$ is less than 30 Hz, the surface feels bumpy as though there existed a row of small solid projections with an interval of a few millimeters. When $f_b$ is greater than 30 Hz but not more than around 100 Hz, the surface feels rough. With an increase of $f_b$, the roughness decreases as though the size and the intervals of the projections became smaller. When $f_b$ is greater than 1 kHz, the surface feels smooth or slippery with low friction.

**Table 1. Scales of the real and virtual objects' roughness.**

| Real Objects (Sandpaper) | | Virtual Objects (Display) | |
|---|---|---|---|
| Number | Scale | fb | Scale |
| #60 | –1.125 | 20 Hz | –1.125 |
| #120 | –0.375 | 40 Hz | –0.5 |
| #240 | 0.375 | 80 Hz | 0.5 |
| #320 | 1.125 | 200 Hz | 1.125 |

### *Evaluation*

We used the paired comparison method for a pilot evaluation of the tactile display. We presented four real objects and four virtual rough objects in the display to five male subjects 25 to 30 years old. The real objects are sandpaper #60, #120, #240, and #320, whose mean radius of projections are 180 µm, 80 µm, 48 µm, and 34 µm, respectively. We presented the virtual rough objects by changing the burst frequency to 20 Hz, 40 Hz, 80 Hz, and 200 Hz. We instructed the subjects to explore the surfaces with their index fingers and compare the roughness of the presented pairs. The subjects evaluated the difference of the roughness of the pairs in five grades. Each subject made 12 comparisons for the real objects and 12 for the virtual objects. Then we constructed scales of the roughness of the real and virtual surfaces by Scheffé's method (see Table 1). The correlation between the scales of the real and the virtual objects is 0.98.

This experiment is a preliminary evaluation, which only shows that the SAW tactile display can produce several distinct sensations that users can subjectively compare the level of roughness such as a bumpy surface with a frequency of 20 Hz and a smooth one with a frequency of 200 Hz. Although the high correlation is due to few stimuli that are far apart, we can consider the qualitative correspondence of the subjective sensation of roughness to the objects' parameters as follows. The variable $f_b$ in the experiment corresponds in the real case to a stick-slip frequency $f_{ss}$. As Figure 5 shows, $f_{ss}$ increases when β, one of the parameters of roughness, decreases. The experimental result that smoothness increases

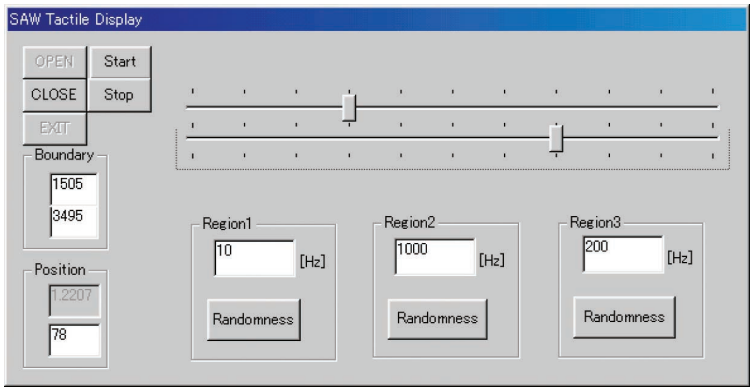


**11** Regions with different granularities of fineness.

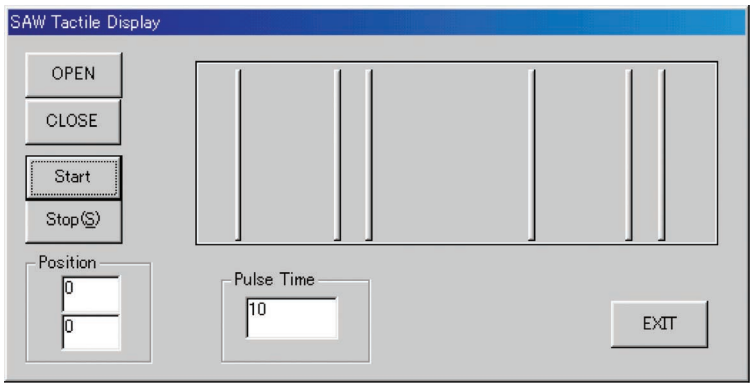


**12** Lines at the designated positions are tangible as though the strings are raised in relief.

when $f_b$ increases justifies this fact. More precisely, as a parameter of the material's quality, we can represent a stick-slip frequency determined by $E\sigma/\beta$ in the SAW tactile display by a burst frequency $f_b$. In future work, we plan to control $f_b$ by Equations 10 through 12 with the parameters measured in real surfaces.

### *Application with position feedback*

By placing a slide rheostat's position sensor with sufficiently low friction on the linear guide, we can generate tactile sensation according to the finger's position.

Figure 11 shows a spatial control application of regions with different granularities of fineness. We divided a region on the screen with the same size as the substrate of the SAW tactile display into three parts—the left, central, and right regions. The buttons on the bars controls the size and position of three regions. By changing the burst frequency in each region, the fineness of the grain changes according to the region. When users explore the SAW tactile display's substrate from the left end to the right, they can feel the regions' level of roughness on the screen by their fingers.

Also, by checking the Randomness button, the burst frequency and the amplitude of the burst signal vary randomly with a designated central burst frequency and central amplitude. By introducing randomness, we can enhance the reality of roughness as if a user explored a surface with fine, randomly distributed scratches.

Figure 12 shows an application of tangible lines on a screen. A mouse cursor moves on the screen according to the motion of a finger on the SAW tactile display. Users can freely choose the number and position of lines. When users explore the position corresponding to a designated line on the screen on the SAW tactile display, a sinusoidal signal modulated by one pulse is applied to the IDTs, which results in creating a sensation of exploring a string raised in relief on the screen. Thus, when users explore the SAW tactile display, they feel as though they have crossed several strings at the designated positions on the screen. Here, we've discovered an interesting phenomenon: when the pulse length gets longer, users perceive two strings. This might be due to the change of friction at the beginning and end of the pulse. By using a triangle wave as a modulation signal, users feel only one string precisely.

## Conclusion

We developed surface acoustic wave tactile display, which can continuously change the fineness of the surface's grain. In the future, by fabricating a 2D position sensor on the substrate of a 3-inch wafer, we'll create a 2D tangible screen that has windows with different levels of roughness and sensible edges in a 2D SAW tactile display. ■

## References


1. R.D. Howe et al., "Remote Palpation Technology," *IEEE Eng. in Medicine and Biology*, vol. 14, no. 3, May/June 1995, pp. 318-323.
2. Y. Ikei et al., "Texture Presentation by Vibratory Tactile Display," *Proc. IEEE Virtual Reality Ann. Int'l Symp.* (VRAIS 96), IEEE CS Press, Los Alamitos, Calif., 1996, pp. 199-205.
3. A. Sato et al., "Development of Non-Constrained Arm with Tactile Feedback Device," *Proc. IEEE Int'l Conf. Advanced Robotics* (ICAR), IEEE Robotics and Automation Soc., Piscataway, N.J., 1991, pp. 334-338.
4. T. Watanabe et. al., "A Method for Controlling Tactile Sensation of Surface Roughness Using Ultrasonic Vibration," *Proc. IEEE Int'l Conf. Advanced Robotics* (ICAR), IEEE Robotics and Automation Soc., Piscataway, N.J., 1995, pp. 1134-1139.
5. R.S Johansson et al., "Tactile Sensory Coding in the Glabrous Skin of the Human Hand," *Trends in Neurosciences*, vol. 6, no. 1, Jan. 1983, pp. 27-32.
6. N. Asamura, N. Yokoyama, and H. Shinoda, "Selectively Stimulating Skin Receptors for Tactile Display," *IEEE Computer Graphics and Applications*, vol. 18, no. 6, Nov./Dec. 1998, pp. 32-37.
7. K.H. Andrew et al., "Morphology of Cutaneous Receptors," *Handbook of Sensory Physiology*, vol. II, Springer-Verlag, Berlin, 1973, p. 16.
8. T. Tachibana et al., "Ultrastructural Localization of Calcium in Mechanoreceptors of the Oral Mucosa," *J. Neurocy-*

*tology*, vol. 21, no. 10, Oct. 1992, pp. 745-753.
9. F. Guharay et al., "Stretch-Activated Single Ion Channel Currents in Tissue-Cultured Embryonic Chick Skeletal Muscle," *J. Physiology*, vol. 352, 1984, pp. 685-701.
10. W. Talbot et al., "The Sense of Flutter-Vibration," *J. Neurophysiology*, vol. 31, no. 2 Mar. 1967, pp. 301-334.
11. T. Nara et al., "Surface Acoustic Wave Tactile Display Based on Properties of Mechanoreceptors," *Proc. IEEE Virtual Reality* (VR2001), IEEE CS Press, Los Alamitos, Calif., 2001, pp. 13-20.
12. M.A. Srinivasan et al., "An Investigation of the Mechanics of Tactile Sense Using Two-Dimensional Models of the Primate Fingertip," *Trans. ASME, J. Biomechanical Engineering*, vol. 118, no. 1, Feb. 1996, pp. 48-55.
13. T. Nara et al., "An Application of SAW to a Tactile Display in a Virtual Reality," *Proc. IEEE Ultrasonics Symp.*, IEEE Press, Piscataway, N.J., 2000, pp. 1-4.
14. V. Hayward et al., "Tactile Display Device Using Distributed Lateral Skin Stretch," *Proc. American Soc. Mechanical Engineers* (ASME), vol. DSC-69-2, American Soc. Mechanical Engineers, New York, 2000, pp. 1309-1314.
15. M. Kurosawa et al., "Ultrasonic Linear Motor Using Surface Acoustic Waves," *IEEE Trans. Ultrasonics, Ferroelectrics, and Frequency Control*, vol. 43, no. 5, Sept. 1996, pp. 901-906.

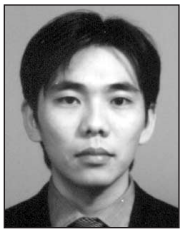

***Takaaki Nara*** *is a research fellow at the Japan Society for the Promotion of Science. His research interests include modeling of processing system of human tactile sensation, development of tactile displays, and analysis of inverse source problems. He has a BE, ME, and PhD in mathematical engineering and information physics from the University of Tokyo.*

***Masaya Takasaki*** *is a research associate at Saitama University. His research interests include SAW devices, ultrasonic motors and magnetic levitation. He has a BE, ME, and PhD in precision machinery engineering from the University of Tokyo.*

***Taro Maeda*** *is an assistant professor at the University of Tokyo. His research interests include psychophysics, modeling of brain by neural networks, man–machine interface for telexistence, and virtual reality. He has a BE and a PhD in mathematical engineering and information physics from the University of Tokyo. He is a member of IEEE, ARVO, and SFN.*

***Toshiro Higuchi*** *is a professor in the Department of Precision Machinery Engineering at the University of Tokyo. His research interests include mechatronics, electrostatic actuators, magnetic bearing, bioengineering, SAW sensors and actuators, and manufacturing. He has a BS, MS, and DrEng in precision machinery engineering from University of Tokyo.*

***Shigeru Ando*** *is a professor in the Department of Information Physics and Computing at the University of Tokyo. He works on research and education on sensors, image processing, optical and acoustic sensing, measurement, and electrical circuits. His interests are on intelligent and smart sensing structure and artificial implementation of sensing and perception of human being. He has a BE, MS, and PhD from the University of Tokyo. He has received the Outstanding Research Award from the Society of Instrument and Control Engineers. He is a member of IEEE, the Optical Society of America, the Acoustical Society of America, the steering committee of Conference of Solid-State Sensors and Actuators (Transducers), the Institute of Electrical Engineers of Japan, the Acoustical Society of Japan, the Optical Society of Japan, and the Society of Instrument and Control Engineers.*

***Susumu Tachi*** *is a professor in the Department of Information Physics and Computing at the University of Tokyo. He is a founding director of the Robotics Society of Japan, a fellow of the Society of Instrument and Control Engineers, and is the president of the Virtual Reality Society of Japan. He also serves as chairman of the International Measurement Confederation (IMEKO) Technical Committee 17 on Measurement in Robotics. His present research covers telexistence, real-time remote robotics (r-cubed), and virtual reality. He has a BE, MS, and PhD in mathematical engineering and information physics from the University of Tokyo.*

*Readers may contact Nara at the Ando Lab., Dept. of Information Physics and Computing, Graduate School of Information Science and Technology, University of Tokyo, 7-3-1, Hongo, Bunkyo-ku, Tokyo, 113-0033, Japan, email nara@alab.t.u-tokyo.ac.jp.*